

A Polymeric Colorimetric Sensor with Excited-State Intramolecular Proton Transfer for Anionic Species

Qinghui Chu, Doug A. Medvetz, and Yi Pang*

Department of Chemistry & Maurice Morton Institute of Polymer Science, The University of Akron,
Akron, Ohio 44325

Received May 23, 2007. Revised Manuscript Received August 22, 2007

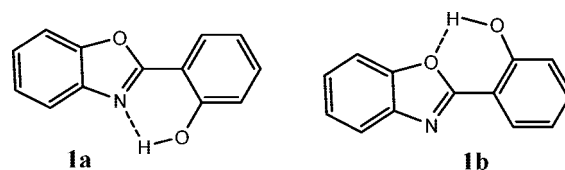
A π -conjugated polymer with 2,5-bis(benzoxazol-2'-yl)benzene-1,4-diol fluorene units is synthesized by using a Suzuki–Miyaura coupling reaction ($M_w = 1.3 \times 10^4$; PDI = 1.8). The polymer exhibits UV–vis absorption, $\lambda_{\max} \approx 421$ nm, and fluorescence, $\lambda_{\max} \approx 616$ nm. The observed large Stokes shift (~ 200 nm) is attributed to an excited-state intramolecular proton-transfer process. The addition of anionic species (hydroxide, fluoride, and acetate) causes the absorption λ_{\max} to be red-shifted to 510–540 nm and the fluorescence quantum efficiency to be increased by a factor of ~ 20 . Through the study of a model compound, the structure of the anion complex is determined to be deprotonated monoanion, as evidenced from the Benesi–Hildebrand plot and electron-spray mass spectrometry. On the basis of a large spectral response in absorption and significant fluorescence enhancement, the material could be useful for dual-channel detection of anions.

Introduction

The use of π -conjugated fluorescent polymers as active media in electroluminescence devices^{1,2} and chemical sensors^{3,4} has been intensively investigated over the past few decades because of their tunable optical properties through rational molecular design. Inclusion of heterocyclic rings along the polymer backbone has been shown to modulate electron affinities and ionization potentials,⁵ which have a direct impact on the charge injection and mobility of materials.

In the chemical sensor area, there are also significant interests in the study of anion-triggered spectral changes in π -conjugated molecules.⁶ Hydrogen-bonding groups such as N–H have been extensively investigated for use as binding sites for anion recognition.^{7,8} Although a large number of small molecules have been shown to be useful for anion sensing, few π -conjugated polymers^{9–12} have been investigated for such applications. Materials with strong absorption and emission in the red or near-IR region are especially of

Scheme 1. Structure of HBO



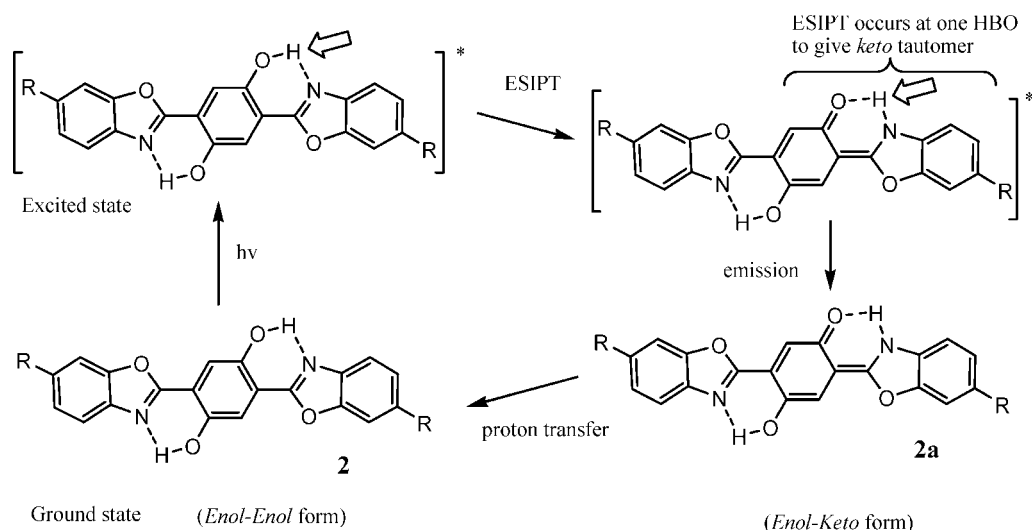
interest because of their high analytical detection limit.¹³ In addition, the autoabsorption of biological matter decreases with the wavelength and is negligible beyond 600 nm.

2-(2-Hydroxyphenyl)-1,3-benzoxazole (HBO; see Scheme 1) derivatives have exhibited interesting colorimetric responses to anions such as halide⁹ and unusually large solvatochromic fluorescence.¹⁴ The intramolecular hydrogen bonding in **1** allows excited-state intramolecular proton transfer (ESIPT) to occur. Studies have demonstrated that the ESIPT process involves transformation from an enol to a keto form and is both solvent-^{15,14} and temperature-¹⁶-dependent. X-ray diffraction of HBO reveals that the intramolecular hydrogen-bonded rotamers **1a** and **1b** exist in about a 1:1 ratio in the crystalline state,¹⁷ with the hydroxyl group pointing to either the N- or O-atom side of the oxazole ring. It has been demonstrated that only conformer **1a** undergoes the ESIPT process,^{18,19} which gives

* Corresponding author.

- (1) Akcelrud, L. *Prog. Polym. Sci.* **2003**, *28*, 875–962.
- (2) Kraft, A.; Grimsdale, A. C.; Holmes, A. B. *Angew. Chem., Int. Ed.* **1998**, *37*, 402–428.
- (3) Thomas, S. W.; Joly, G. D.; Swager, T. M. *Chem. Rev.* **2007**, *107*, 1339–1386.
- (4) Toal, S. J.; Trogler, W. C. *J. Mater. Chem.* **2006**, *16*, 2871–2883.
- (5) Zhang, X.; Jenekhe, S. A. *Macromolecules* **2000**, *33*, 2069–2082.
- (6) Martínez-Mañez, R.; Sancenon, F. *Chem. Rev.* **2003**, *103*, 4419–4476.
- (7) Amendola, V.; Esteban-Gómez, D.; Fabbri, L.; Licchelli, M. *Acc. Chem. Rev.* **2006**, *39*, 343–353.
- (8) Gale, P. A. *Acc. Chem. Res.* **2006**, *39*, 465–475.
- (9) Lee, J. K.; Na, J.; Kim, T. H.; Kim, Y.-S.; Park, W. H.; Lee, T. S. *Mater. Sci. Eng., C* **2004**, *C24*, 261–264.
- (10) Zhou, G.; Cheng, Y.; Wang, L.; Jing, X.; Wang, F. *Macromolecules* **2005**, *38*, 2148–2153.
- (11) Wu, C.-Y.; Chen, M.-S.; Lin, C.-A.; Lin, S.-C.; Sun, S.-S. *Chem.—Eur. J.* **2006**, *12*, 2263–2269.
- (12) Aldakov, D.; Anzenbacher, P. *J. Am. Chem. Soc.* **2004**, *126*, 4752–4753.

- (13) *Near-Infrared Dyes for High Technology Applications*; Daehne, S., Resch-Genger, U., Wolfbeis, O. S., Eds.; Kluwer Academic: Boston, 1997.
- (14) Seo, J.; Kim, S.; Park, S. Y. *J. Am. Chem. Soc.* **2004**, *126*, 11154–11155.
- (15) Abou-Zied, O. K.; Jimenez, R.; Thompson, E. H. Z.; Millar, D. P.; Romesberg, F. E. *J. Phys. Chem. A* **2002**, *106*, 3665–3672.
- (16) Das, K.; Sarkar, N.; Ghosh, A. K.; Majumdar, D.; Nath, D. N.; Bhattacharyya, K. *J. Phys. Chem.* **1994**, *98*, 9126–9132.
- (17) Tong, Y. P. *Acta Crystallogr., Sect. E* **2005**, *61*, o3076–o3078.
- (18) Woolfe, G. J.; Melzig, M.; Schneider, S.; Doerr, F. *Chem. Phys.* **1983**, *72*, 213–221.
- (19) Das, K.; Sarkar, N.; Majumdar, D.; Bhattacharyya, K. *Chem. Phys. Lett.* **1992**, *198*, 443–448.

Scheme 2. Schematic Representation of the ESIPT Process in Bis(HBO)^a

^a The double arrow points to the proton that undergoes the ESIPT process.

rise to the emission with a large Stokes shift. It is thus desirable to minimize the content of **1b** for optimal performance of the ESIPT-based HBO sensor system.

2,5-Bis(benzoxazol-2'-yl)benzene-1,4-diol derivative **2**, bis(HBO) (see Scheme 2), represents an interesting system to study, in which two benzoxazole units are locked into a coplanar structure (or fused ring) through intramolecular hydrogen bonding with adjacent hydroxyl groups. Polymers with such a structural unit have exhibited useful properties, which include great thermal stability ($T_g > 450$ °C)²⁰ and unique fluorescent patterning.²¹ The presence of two reactive sites in **2** for ESIPT provides an additional option to tune the molecular response toward various chemical species. In the ground state of **2**, both HBO groups are in the *enol* form. It is likely that one of the HBO groups in the excited state undergoes the ESIPT process, as a double proton transfer remains a debated issue.²² This leads to the *enol-keto* structure **2a**, which emits a photon with a large Stokes shift. It should be noticed that the *enol* part in **2a** remains to be coplanar with the *keto* structure (via hydrogen bonding), which directly influences the emission property of the HBO chromophore. Such electronic perturbation at the ESIPT site on the HBO chromophore would shift the emission to a longer wavelength, thereby tuning the emission to the desirable red or near-IR region. Several studies have been reported to include a mono(HBO) group along the polymer main^{9,23,24} and side²⁵ chains. A polymer²¹ containing a bis(HBO) functional group, which is only soluble in strong

acid, has shown orange fluorescence (with contribution from both *enol* and *keto* forms) and interesting photopatterning properties. In this report, we describe the synthesis of a bis(HBO)-containing π -conjugated polymer **5**, which exhibits enhanced fluorescence upon interaction with anionic species.

Results and Discussion

Polymer Synthesis and Characterization. The key building block **3** was assembled by condensation of a dialdehyde with 2.0 equiv of *o*-aminophenol, followed by cyclization under oxidative conditions. Coupling of monomer **3b** with fluoreneboronic ester (Suzuki–Miyaura coupling²⁶) gave polymer **4** with $M_w = 1.3 \times 10^4$ (PDI = 1.8). The polymer structure was confirmed by NMR and elemental analysis data. The desirable **5** was obtained by treatment of **4** with BBR_3 , which quantitatively removed the alkyl protecting groups as observed from the ¹H NMR spectrum (absence of a signal at ~ 4.3 ppm for $-\text{OCH}_2-$). The free hydroxyl proton in **5** gave a characteristic sharp NMR resonance at 11.1 ppm. The ¹H NMR signal for the aromatic proton H_a in **5** occurred at 8.08 ppm as a well-resolved singlet (Figure S2 in the Supporting Information). The 1:1 ratio between signals at 11.1 and 8.08 ppm further indicated that the conversion was complete. The IR spectrum of **5** in KBr pellets (Figure S4 in the Supporting Information) revealed a broad absorption band at ~ 3200 cm^{-1} , indicating the formation of an intramolecular hydrogen bonding.²⁷

Optical Properties. Polymer **4** in tetrahydrofuran (THF) exhibited absorption λ_{max} at 329 and 381 nm and intense blue fluorescence at 425 and 449 nm with $\phi_{\text{fl}} = 0.69$ (Figure 1). Removal of alkyl protecting groups gave weakly fluorescent **5** with a fluorescent quantum yield of $\phi_{\text{fl}} \approx 0.023$. The emission peak of **5**, however, was red-shifted from that of **4** by ~ 200 nm (to $\lambda_{\text{max}} = 616$ nm), in contrast to a much

(20) Dang, T. D.; Mather, P. T.; Alexander, M. D., Jr.; Grayson, C. J.; Houtz, M. D.; Spry, R. J.; Arnold, F. E. *J. Polym. Sci., Part A: Polym. Chem.* **2000**, *38*, 1991–2003.

(21) Park, S.; Kim, S.; Seo, J.; Park, S. Y. *Macromolecules* **2005**, *38*, 4557–4559.

(22) Weib, J.; May, V.; Ernsting, N. P.; Farztdinov, V.; Mühlpfordt, A. *Chem. Phys. Lett.* **2001**, *346*, 503–511.

(23) Lee, J. K.; Kim, H.-J.; Kim, T. H.; Lee, C.-H.; Park, W. H.; Kim, J.; Lee, T. S. *Macromolecules* **2005**, *38*, 9427–9433.

(24) Lee, J. K.; Lee, T. S. *J. Polym. Sci., Part A: Polym. Chem.* **2005**, *43*, 1397–1403.

(25) Campo, L. F.; Rodembusch, S. F.; Stefani, V. *J. Appl. Polym. Sci.* **2006**, *99*, 2109–2116.

(26) Miyaura, N.; Suzuki, A. *Chem. Rev.* **1995**, *95*, 2457–2483.

(27) Lin-Vien, D.; Colthup, N. B.; Fateley, W. G.; Grasselli, J. G. *The Handbook of Infrared and Raman Characteristic Frequencies of Organic Molecules*; Academic Press, Inc.: Boston, 1991.

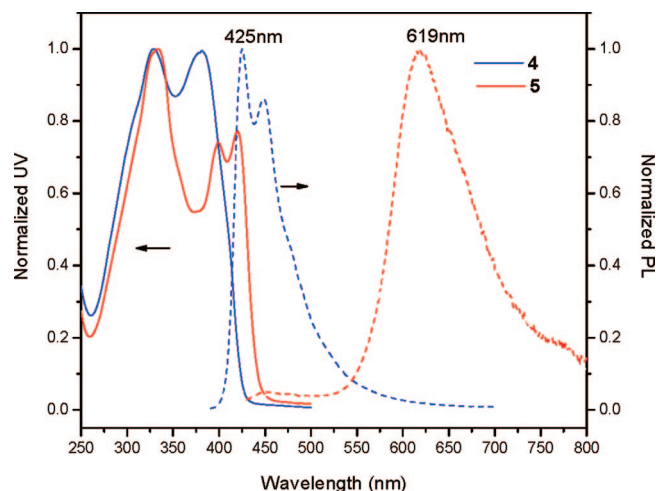


Figure 1. Absorption (solid line) and emission (dotted line) of polymers **4** (blue) and **5** (red) in anhydrous THF.

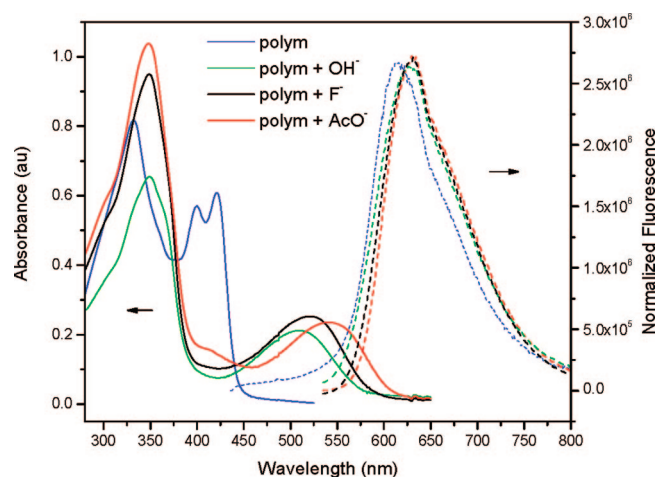


Figure 2. UV-vis (solid line) and fluorescence (broken line) spectra of polymer **5** and its anionic complexes.

smaller bathochromic shift (~ 40 nm) in absorption. The large Stokes' shift (~ 200 nm) was attributed to the ESIPT process occurring in the bis(HBO) chromophore of **5**, which is not available in **4**. In comparison with the known π -conjugated polymer containing the mono(HBO) group,⁹ which exhibits emission at ~ 518 nm, the bis(HBO)-containing polymer exhibits a notable advantage by extending the emission to a longer wavelength (by ~ 100 nm).

The absorption of **5** in THF exhibited a relatively high energy band at 332 nm and low energy bands at 400 and 421 nm (Figure 2). Upon the addition of anionic species (OH^- , F^- , and AcO^-), a new absorption band occurred instantly at 510–540 nm, accompanied with a visible color change to red. In addition, the characteristic structured absorption bands at 400 and 421 nm decreased almost completely, suggesting that significant electronic perturbation occurred in the ground state of bis(HBO). Different absorption λ_{max} values were observed for different anionic species (Table 1), allowing one to distinguish them on the basis of their own electronic signatures. Titration of **5** with $\text{Bu}_4\text{N}^+\text{OAc}^-$ (a weaker base) in THF caused the absorption band to be red-shifted by as much as 120 nm (to $\lambda_{\text{max}} = 541$ nm). The results clearly showed that the bis(HBO) group was a useful receptor for anions.

Table 1. Photophysical Properties of Polymer **5**, Model Compound **6**, and Their Anionic Complexes

compound	$\lambda_{\text{max,abs}}$ (nm)	$\lambda_{\text{max,PL}}$ (nm)	quantum ratio ^a	$\Phi_{\text{fl, sol}}$
5	330, 400, 421	616		0.023 ^b
5-OH⁻	510	628	6	0.14 ^c
5-F⁻	521	631	7	0.16 ^c
5-AcO⁻	541	632	4	0.092 ^c
6	392, 412	607		0.021 ^b
6-OH⁻	496	601	8	0.17 ^c
6-F⁻	518	615	19	0.40 ^c
6-AcO⁻	532	620	18	0.38 ^c

^a The quantum ratio was measured by a comparison of the emission intensity (integrated area) of anion complexes with that of the sensor excitation at isosbestic absorbance. ^b The quantum yield was measured by a comparison with that of quinine sulfate in 0.1 M H_2SO_4 . ^c The quantum yield was calculated from the measured quantum yield and quantum ratio.



Figure 3. Emission of polymer **4** (left), **5** (middle), and **5+F⁻** (right) in THF/ethanol (50:1 ratio) under UV irradiation (365 nm).

The relatively low φ_{fl} value observed from **5** is associated with the bis(HBO) molecular fragment, which is known to have a low fluorescence quantum yield.²⁸ An interesting question is whether the energy pool accumulated at the bis(HBO) unit can be redirected to photoluminescence by electronic perturbation of the structural unit. To test this hypothesis, fluorescence signals were monitored upon the addition of anions. Interestingly, the addition of fluoride or acetate anions drastically raised the fluorescence intensity by a factor of ~ 20 (Figure 3 and Table 1). The presence of the anions caused a bathochromic shift of the emission band by ~ 15 nm, in sharp contrast to the large red shift (as large as 120 nm) observed in their absorption spectra. The excitation spectra for **5** and its anionic complexes (Figure 4) resembled their respective absorption spectra, showing that the enhanced emission from the molecular anionic complexes originated indeed from their new absorption band at about 500–550 nm. The anion-triggered fluorescence turn-on in the bis(HBO)-containing chromophore, therefore, can be achieved through proper analyte interaction in the ground state.

Model Compound Study. Poor solubility of polymer **5** put the limitation on its characterization. To gain a further understanding about the intriguing optical response of the bis(HBO) unit, a model compound **6** was prepared similarly from **3b** (Scheme 3). The crystal structure of **6** (Figure 5) confirmed that both hydroxyl groups were oriented to form an intramolecular O–H \cdots N hydrogen bond with the adjacent oxazole rings. The hydrogen bond length for H \cdots N in

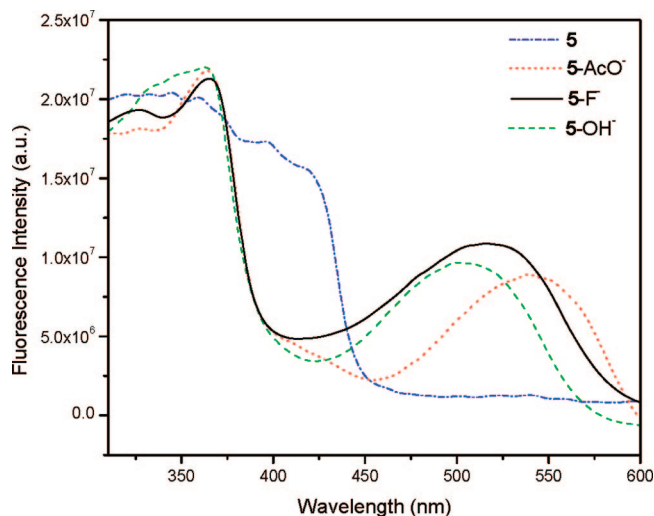


Figure 4. Excitation spectra of polymer **5** while monitoring the emission at ~ 620 nm.

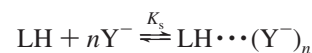
6 is 1.888 \AA , which is notably shorter than that in mono-(HBO) **1a** (1.97 \AA).¹⁷ Each HBO group in **6** adopts the rotamer conformation of **1a**, which provides an ideal molecular geometry for the ESIPt process. The observation of an O–H \cdots O hydrogen bond in **1** (as seen in **1b**) but not in **6**, in addition to the shorter H \cdots N bond distance, suggests that the O–H \cdots N bond is energetically more favorable in the latter than in the former. The known intermolecular hydrogen bond strength²⁹ for O–H \cdots N ($\Delta H = -6.5$ kcal/mol, measured from phenol/pyridine) is comparable with that for the O–H \cdots O bond ($\Delta H = -5.0$ kcal/mol, measured from phenol/ether). The exclusive formation of the O–H \cdots N bond in **6**, in sharp contrast to the 1:1 ratio of O–H \cdots N to O–H \cdots O in **1**,¹⁷ could be attributed to the cooperative interaction of two intramolecular hydrogen bonds in the para position.

The absorption spectra of **6** were recorded upon the addition of $\text{Bu}_4\text{N}^+\text{OH}^-$ (Figure 6). A new absorption band occurred at 496 nm, and its intensity gradually increased along with decreasing absorbance at 412 nm. With the addition of sufficient base, the characteristic absorption bands at 400 and 410 nm were completely shifted to longer wavelength, indicating that all neutral hydrogen-bonded bis(HBO) molecules were consumed. All spectra intersected at one wavelength (~ 432 nm), forming a characteristic *isosbestic* point. The result suggested that *only* one new chemical species was formed during the titration. Semiempirical ZINDO calculations predicted about a 100 nm red shift in absorption λ_{max} when **6** was changed to its monoanion, supporting the assumption that the colorimetric response was due to the O–H deprotonation of **6**. The bathochromic shift of 84 nm (from 412 to 496 nm) was apparently due to the enhanced π -electron delocalization upon deprotonation. Although the absorption peak at 500 nm continued to increase with the **6**: OH^- ratio (from 1:1 to 1:2), there was

no new peak formed in the spectra (Figure 6), which favors the monoanion formation.

A solution of **6** in CDCl_3 was monitored by ^1H NMR as Bu_4NOH in CD_3OD was added. The signals at ~ 7.8 ppm (Figure 7) were attributed to two overlapping singlet aromatic protons (H_a and H_b as labeled in the structure of **6**). The resonance signals were slightly drifted toward the upper field, attributed to interaction with both the methanol solvent and hydroxide anion. The difference between protons H_a and H_b became visible in the presence of base because the anion formation (through deprotonation of the hydroxyl group) would exert more influence on the aromatic proton of the central benzene ring (proton H_a). The magnitude of the signal splitting between H_a and H_b increased with the OH^- :**6** ratio (from 0:1 to 0.8:1). The addition of a second 1 equiv of hydroxide resulted in neither additional splitting nor significant line broadening, suggesting that the monoanion or **6**: OH^- complex was likely to be formed under those conditions.

Determination of the Stoichiometry and Stability Constants of the Complexes. The complex formation between a proton donor LH and an anion is characterized by the following equilibrium:



The complex formation constant K_s can be expressed as

$$K_s = \frac{[\text{LH}\cdots(\text{Y}^-)_n]}{[\text{LH}][\text{Y}^-]^n} = \frac{[\text{LH}\cdots(\text{Y}^-)_n]}{(c_0 - [\text{LH}\cdots(\text{Y}^-)_n])[\text{Y}^-]^n}$$

where c_0 is the total concentration of the proton donor (LH) and its anionic complex ($\text{LH}\cdots\text{Y}^-$) in equilibrium $c_0 = [\text{LH}] + [\text{LH}\cdots\text{Y}^-]_n$. This is in agreement with the spectroscopic evidence that only one new species formed in the equilibrium. Substitution of the concentration with absorbance ($A = \epsilon[\text{C}]$), followed by rearrangement, leads to the Benesi–Hildebrand equation³⁰ shown below, which is used to estimate the ratio of chromophore–anion association.³¹

$$\frac{A_0}{A - A_0} = \frac{\epsilon_{\text{LH}}}{\epsilon_{\text{LH}\cdots\text{Y}^-} - \epsilon_{\text{LH}}} \left(\frac{1}{K_s[\text{Y}^-]^n} + 1 \right)$$

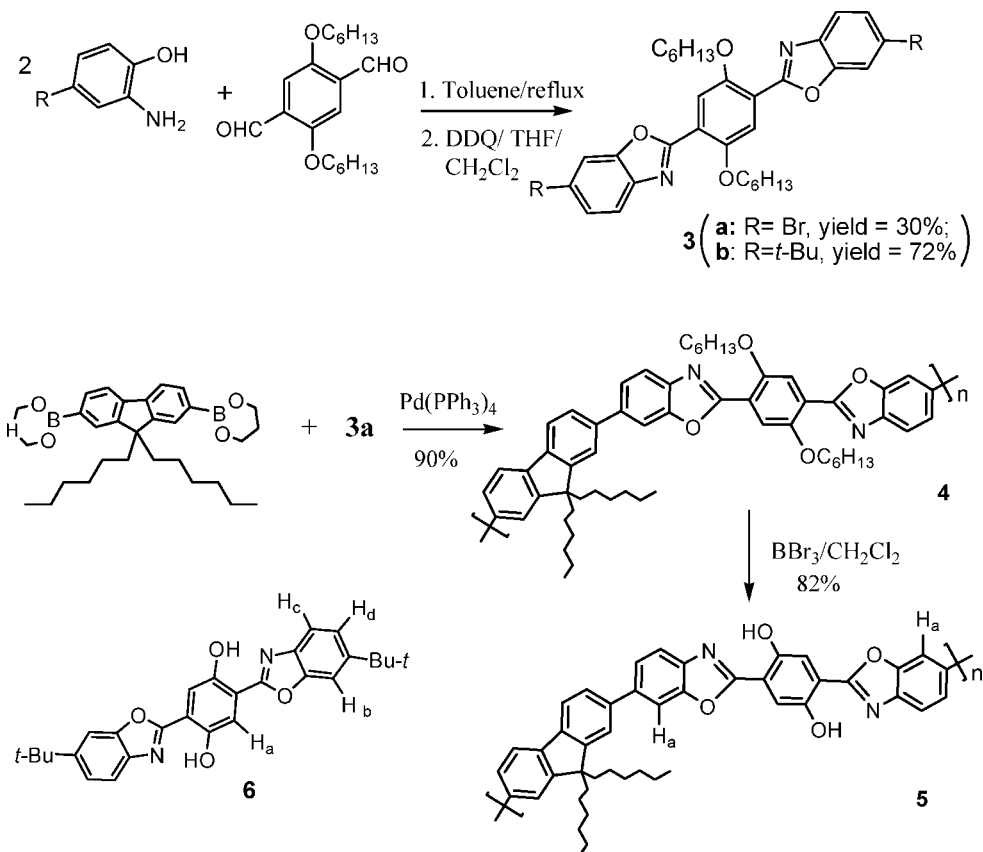
Plotting the $A_0/(A_0 - A)$ quantity against $1/c_{\text{AcO}^-}$ by using absorbance at 412 nm gave an excellent linear fit (the Benesi–Hildebrand plot in Figure 8), showing that the composition of the complex had a 1:1 ratio for **6** and the acetate anion. This result suggested that only one of the two hydroxyl groups was interacting with or deprotonated by the acetate anion. The resulting monoanion **6**[−] appeared to refuse further interaction with the excess acetate anion, largely attributing to the Coulombic repulsion between the negatively charged species. The complex constant was calculated to be $K_s = 133$, indicating that the bis(HBO) chromophore is not very effective in interacting with the acetate anion.

(29) (a) Selected hydrogen bond strength can be found in: Anslyn, E. V.; Dougherty, D. A. *Modern Physical Organic Chemistry*; University Science Books: Herndon, VA, 2006; pp 171–80. (b) Selected hydrogen bond strength can be found in: Joesten, M. D.; Schaad, L. J. *Hydrogen Bonding*; Marcel Dekker: New York; 1974.

(30) Benesi, H. A.; Hildebrand, J. H. *J. Am. Chem. Soc.* **1949**, *71*, 2703–2707.

(31) Connors, K. A. *Binding Constants: The Measurement of Molecular Complex Stability*; John Wiley & Sons: New York, 1987.

Scheme 3. Synthesis of Polymer 5 and Its Model Compound 6



Titration of **6** with Bu_4NF revealed that the presence of excess fluoride anions was also necessary for the

complex formation (Figure 9). The spectra exhibited one isosbestic point at $\sim 433 \text{ nm}$, attributed to a newly formed chemical species. The Benesi–Hildebrand plot, however,

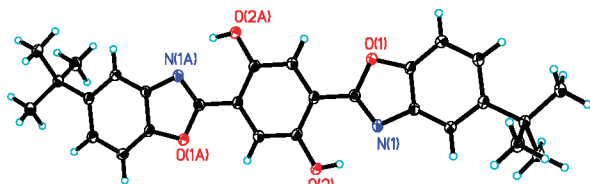


Figure 5. Crystal structure of **6** shows that both hydroxyl groups are hydrogen-bonded to N-atom of oxazole rings.

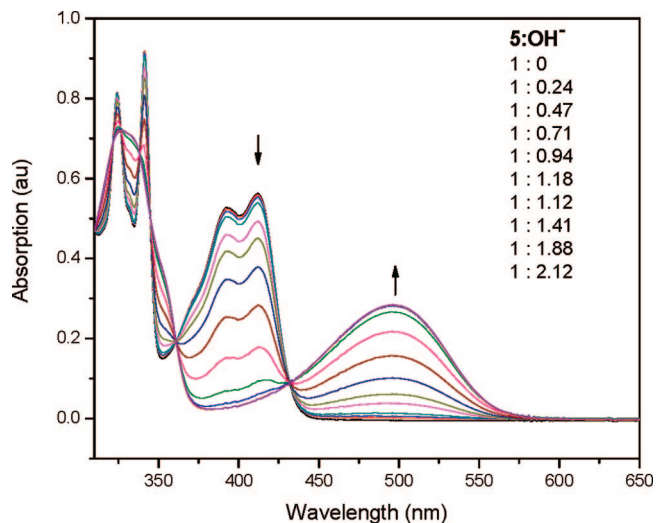


Figure 6. Titration spectra of model compound **6** with Bu_4NOH in the mixture of THF and EtOH (30:1).

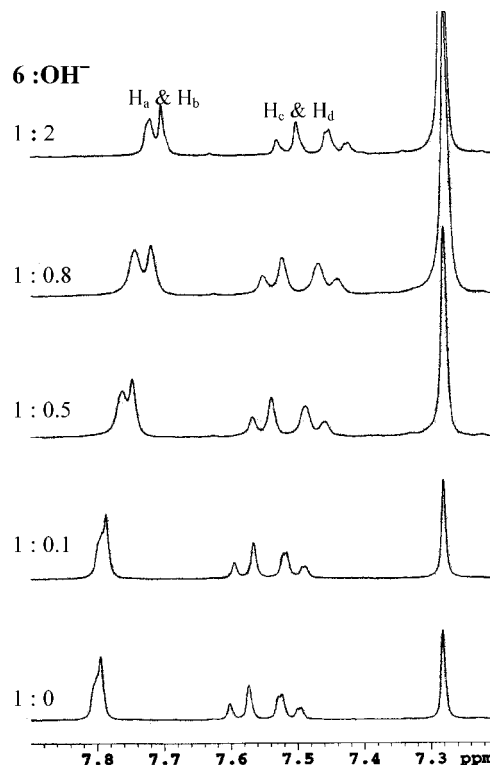


Figure 7. ^1H NMR spectra of **6** in CDCl_3 with the addition of Bu_4NOH in CD_3OD . The signal at 7.27 ppm is attributed to the CHCl_3 residue.

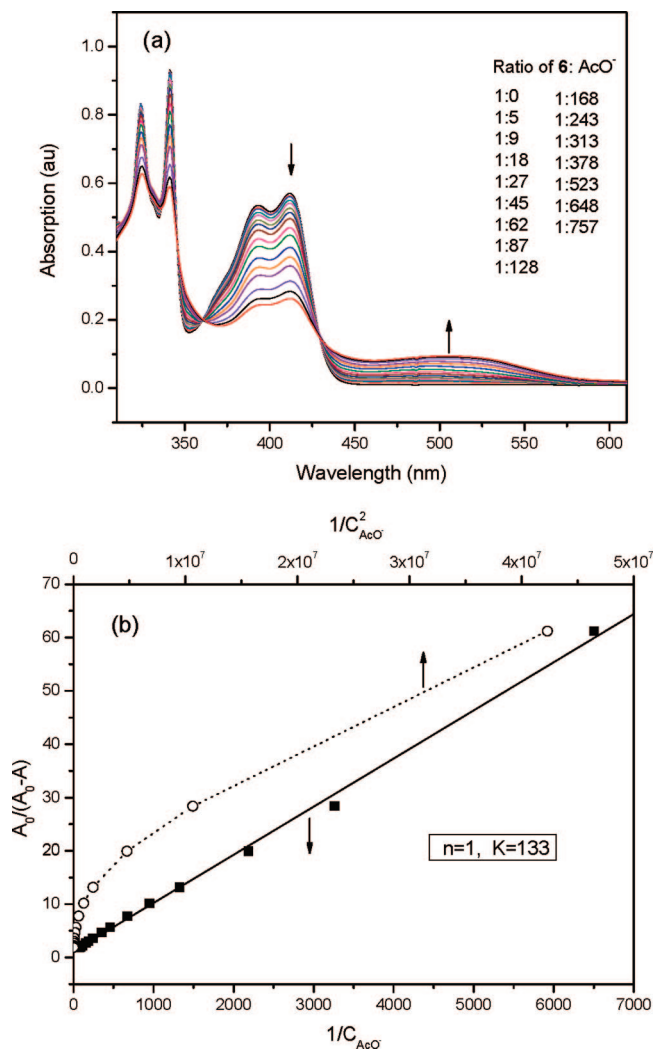


Figure 8. (a) UV-vis absorption spectra of **6** titrated with Bu_4NOAc in THF (top). (b) Benesi-Hildebrand plot for complexation of **6** with the acetate anion (bottom), where the solid line is fitted with 1:1 complexation and the dotted line is fitted with 1:2 complexation.

showed that the complex involved two fluoride anions, in contrast to that observed with the acetate anion. The stronger hydrogen-bonding capability of fluoride could account for its higher binding ratio and larger complex constant with **6** ($K_s = 1.1 \times 10^7$).

Spectral evidence suggests the formation of monoanionic species because only one isosbestic point is observed in the titration. Possible structures for the anion are **7** and **8**, where a partial hydrogen bonding between the anion (Y^-) and HBO remains in the former. Both structures **7** and **8** are consistent with the Benesi-Hildebrand plot observed from titration of **6** with the acetate anion. In the titration with the fluoride anion, the Benesi-Hildebrand plot suggests the involvement of two fluorides in the anion formation process. This is in agreement with the formation of a $[\text{F} \cdots \text{H} \cdots \text{F}]^-$ byproduct during the monoanion formation, which is typical in the fluoride-induced deprotonation process.^{11,32} A likely mechanism is that the first F^- anion interacts with **6** through hydrogen bonding to form **7** ($\text{Y}^- = \text{F}^-$), while the second F^- anion induces deprotonation to form the $[\text{HF}_2]^-$ ion.

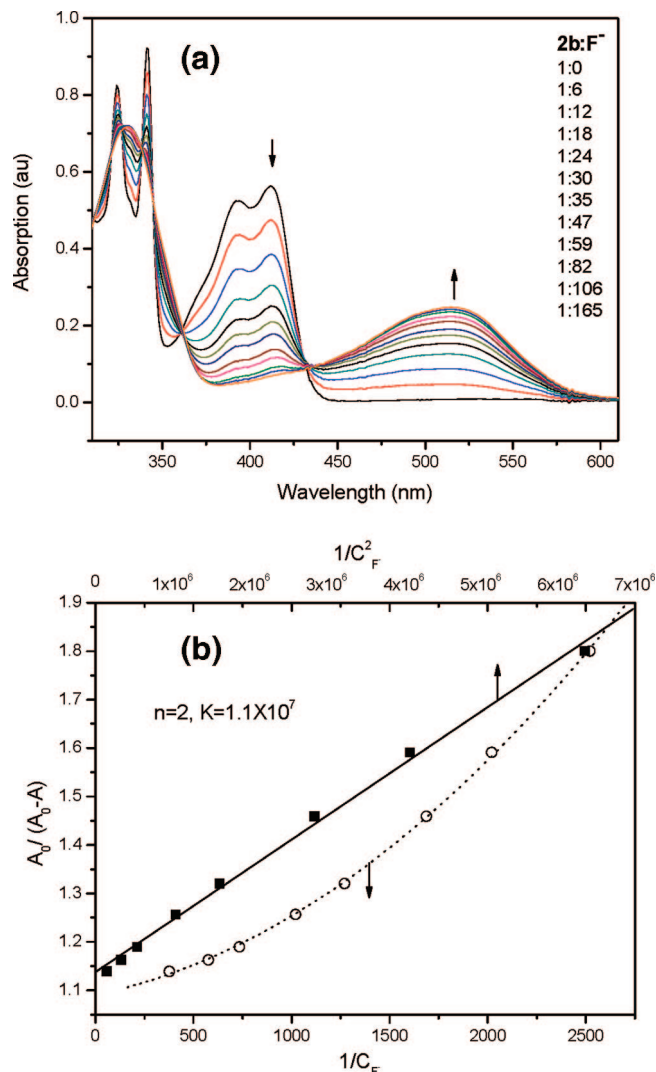


Figure 9. Titration spectra and Benesi-Hildebrand plot of **6** with Bu_4NF in a mixture of THF and EtOH (100:1).

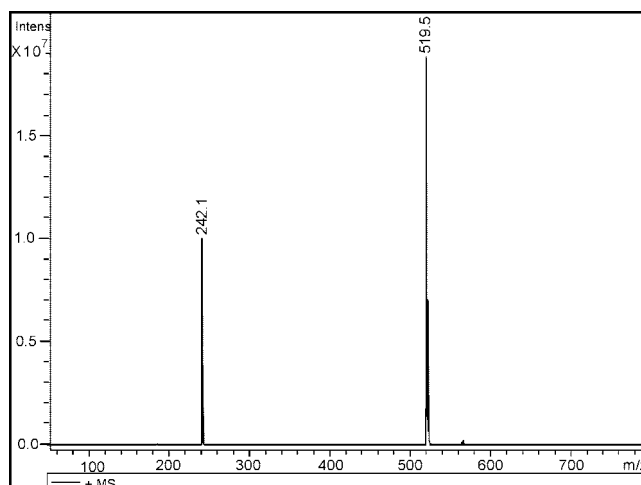
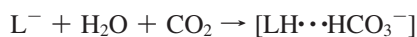
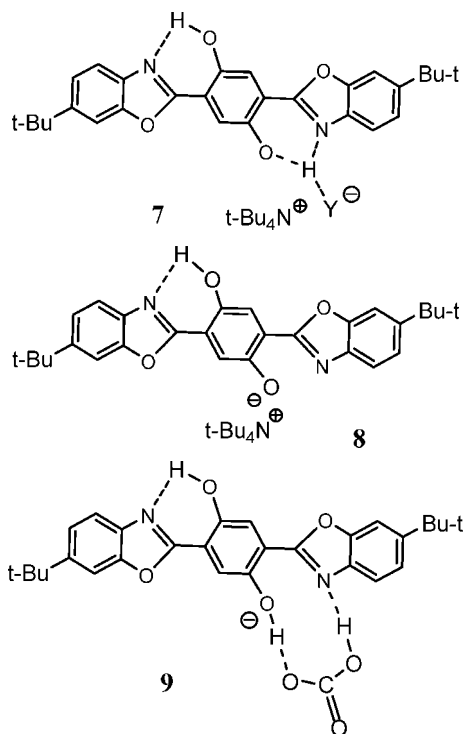


Figure 10. ESI-MS spectrum of **6** and $(\text{Bu}_4)\text{NOH}$, acquired under HAC flow.

To further confirm the structure, the product solution from **6** and Bu_4NOH was subjected to analysis by using electrospray ionization tandem mass spectrometry (ESI-MS). Molecular masses at m/z 455.4 and 473.3 were detected by using the negative-mode electrospray, suggesting the presence of

(32) Peng, X.; Wu, Y.; Fan, J.; Tian, M.; Han, K. *J. Org. Chem.* **2005**, *70*, 10524-10531.

monoanion **8** and **8**·H₂O, respectively. With the positive-mode electrospray under acetic acid flow, the spectrum detected two peaks (Figure 10) with mass at *m/z* 242.1 attributed to the (Bu)₄N⁺ cation. The mass of *m/z* 519.5 was assigned to a molecular complex [LH···HCO₃⁻], which was detected as a protonated cation under acetic acid flow. The anionic complex with HCO₃⁻ (**9**), which is precedent with a urea anion,³³ is produced by reaction of the anion **8** (L⁻) with carbon dioxide from air in the presence of water as shown below:



Solvatochromic Effect. The fluorescence spectra of **6** in different solvents exhibited little solvatochromic effect (Figure 11). It is known that a HBO molecule gives emission from both *enol* and *keto* tautomers, and their ratio represents the relative efficiency of the ESIPT process.¹⁶ The emission signal from **6** is overwhelmingly from the *keto* tautomer at ~600 nm in both nonpolar and polar (e.g., EtOH) solvents. The weak emission peak at ~425 nm is from the *enol* tautomer (without ESIPT). This is in sharp contrast to the mono(HBO) system, where a strong solvatochromic fluorescence has been reported in methanol.¹⁴ Less emission from the *enol* tautomer of **6** suggests that the ESIPT process occurs with ease in the bis(HBO) system, and its implication in sensor applications awaits to be explored. Weaker solvent effects on the fluorescence of the bis(HBO) system is apparently associated with its stronger hydrogen bonding.

Conclusion

A π -conjugated polymer with 2,5-bis(benzoxazol-2'-yl)-benzene-1,4-diol and fluorene units has been synthesized and characterized. The polymer exhibits UV-vis absorption λ_{\max}

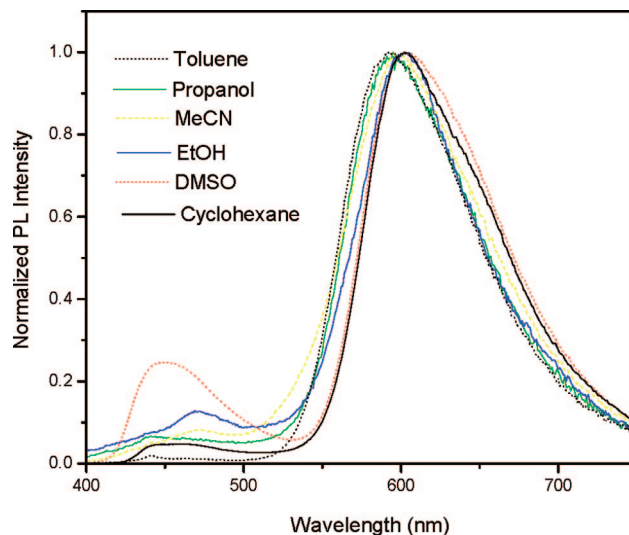


Figure 11. Fluorescence spectra of **6** at 25 °C in different solvents.

≈ 421 nm and fluorescence $\lambda_{\max} \approx 616$ nm, displaying a large Stokes shift (~200 nm) as a result of the ESIPT process. The addition of anionic species (hydroxide, fluoride, and acetate) causes the absorption λ_{\max} to be red-shifted by as much as 120 nm to 510–540 nm and raises the fluorescence quantum efficiency by a factor of ~20. Large spectral responses in both absorption and emission indicate the potential of the bis(HBO) chromophore in sensor applications. In comparison with the known mono(HBO) system, where the anion-induced absorption is at ~420 nm,⁹ the bis(HBO) chromophore shifts both absorption and emission to longer wavelength by more than 100 nm, which is desirable for detection in biological systems. The great fluorescence turn-on, in addition to its red emission, shows that the bis(HBO) chromophore exhibits anionic sensing properties superior to those of the mono(HBO) analogue. It is likely that the anionic species significantly perturbs the hydrogen-bonding structure in the bis(HBO) fragment, thereby affecting the radiative decay rate (or process) and increasing the fluorescence intensity.

Through the study of a model compound, the structure of the anion complex is determined to be deprotonated monoanion **8**, as evidenced from ESI-MS and ¹H NMR. The proposed anionic structure is consistent with that concluded from the Benesi-Hildebrand plot, which indicates that 1 equiv of the acetate anion is involved in the anion complexation. It appears that in the bis(HBO) sensor only one of the two HBO groups is utilized to interact with the analyte species. This leaves the second HBO for other potentially useful functions. Stronger hydrogen bonding in bis(HBO), in comparison with the mono(HBO) system, is attributed to greater stability. Spectral similarity between **5** and **6** in responding to anionic species (Table 1) indicates that the bis(HBO) fragment is largely responsible for the interesting optical behavior in the polymer. The fluorene units attached to the bis(HBO) chromophore appear to extend conjugation slightly to longer wavelength (by ~10 nm in absorption). When the polymer responds to anionic species, the formation of a monoanion is believed to occur similarly on the bis(HBO) subunit. A further study is in progress to understand the scope and limitation of the bis(HBO) sensor system

(33) Boiocchi, M.; Boca, L. D.; Gómez, D. E.; Fabbrizzi, L.; Licchelli, M.; Monzani, E. *J. Am. Chem. Soc.* **2004**, *126*, 16507–16514.

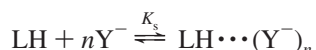
and to evaluate the chromophore behavior in different environments.

Experimental Section

Materials and General Procedures. 2-Amino-4-*tert*-butylphenol, 9,9-dihexylfluorene-2,7-bis(trimethyleneborate), 9,9-dioctethylfluorene-2,7-bis(trimethyleneborate), 2,5-bis(hexyloxy)teraphthalaldehyde, and Pd(PPh₃)₄ were purchased from Aldrich, and DDQ and other chemicals were from Acros. 2-Amino-4-bromophenol was prepared from 4-bromo-2-nitrophenol by using a modified literature procedure.³⁴ Anhydrous THF solvent, which was freshly distilled over sodium, was used in both absorption and fluorescence studies. Toluene, dimethyl sulfoxide, ethanol, and acetonitrile of extrady grade were received from Acros or Fisher and were used in a solvatochromic study without further purification. NMR spectra were collected on a Varian 300 Gemini spectrometer. UV-vis spectra were acquired on a Hewlett-Packard 8453 diode-array spectrophotometer and a Perkin-Elmer Lambda 950 UV-vis spectrophotometer. Fluorescence spectra were obtained on a HORIBA Jobin Yvon NanoLog spectrofluorometer. The slit width was set at 2 nm for both excitation and fluorescence spectra. The quantum yields were measured in a THF solvent, by using quinine sulfate as the standard ($\varphi_{fl} = 0.53$, at 366 nm).³⁵ Size-exclusion chromatography (SEC) analysis was performed on a Waters 510 system equipped with three Waters styragel high-resolution columns (a single-porosity column HR1 100 Å and two mixed-porosity columns HR4E and HR5E with 50, 500, 10³, 10⁴, 10⁵, and 10⁶ Å), a Waters 410 differential refractometer, and a Wyatt Dawn EOS multiangle-laser light-scattering (MALLS) detector. The experiments were carried out in THF at 35 °C at a flow rate of 1.0 mL/min. The results were analyzed by using Wyatt ASTRA v4 software. X-ray crystallography data were measured on a Bruker SMART APEX CCD-based X-ray diffractometer system equipped with a Mo-target X-ray tube ($\lambda = 0.71073$ Å) operated at 2000 W power.

Semiempirical ZINDO calculation of **5** was performed to estimate the highest occupied molecular orbital–lowest unoccupied molecular orbital gap and the corresponding electronic absorption λ_{max} . The structure was first optimized by using a semiempirical AM1 method with a HyperChem software package.³⁶

Determination of the Stoichiometry and Stability Constants of the Complexes. For the chemical equilibrium



the complex formation constant K_s can be expressed as

$$K_s = \frac{[\text{LH}\cdots(\text{Y}^-)_n]}{[\text{LH}][\text{Y}^-]^n} = \frac{[\text{LH}\cdots(\text{Y}^-)_n]}{(c_0 - [\text{LH}\cdots(\text{Y}^-)_n])[\text{Y}^-]^n} \quad (1)$$

where c_0 is the total concentration of the proton donor (LH) and its anionic complex (LH \cdots Y[−]) in equilibrium, i.e., $c_0 = [\text{LH}] + [\text{LH}\cdots(\text{Y}^-)_n]$. This is in agreement with the spectroscopic evidence that only one new species formed in the equilibrium. The absorbance A of the solution at a specific wavelength λ is thus given by

$$A = \epsilon_{\text{LH}}c_{\text{LH}} + \epsilon_{\text{LH-Y}}c_{\text{LH-Y}} = \epsilon_{\text{LH}}(c_0 - c_{\text{LH-Y}}) + \epsilon_{\text{LH-Y}}c_{\text{LH-Y}} = \epsilon_{\text{LH}}c_0 + (\epsilon_{\text{LH-Y}} - \epsilon_{\text{LH}})c_{\text{LH-Y}} \quad (2)$$

Therefore,

$$c_{\text{LH-Y}} = (A - \epsilon_{\text{LH}}c_0) / (\epsilon_{\text{LH-Y}} - \epsilon_{\text{LH}})$$

After the expression is substituted for $c_{\text{LH-Y}}$ in equation 1, we have

$$\frac{1}{K_s[\text{Y}^-]^n} = \frac{c_0}{[\text{LH}\cdots(\text{Y}^-)_n]} - 1 = \frac{c_0(\epsilon_{\text{LH}\cdots\text{Y}^-} - \epsilon_{\text{LH}})}{A - \epsilon_{\text{LH}}c_0} - 1$$

$$\frac{1}{K_s[\text{Y}^-]^n} + 1 = \frac{\epsilon_{\text{LH}\cdots\text{Y}^-} - \epsilon_{\text{LH}}}{\epsilon_{\text{LH}}} \frac{c_0\epsilon_{\text{LH}}}{A - \epsilon_{\text{LH}}c_0} = \frac{\epsilon_{\text{LH}\cdots\text{Y}^-} - \epsilon_{\text{LH}}}{\epsilon_{\text{LH}}} \frac{A_0}{A - A_0}$$

Here $A_0 = \epsilon_{\text{LH}}c_0$, which is the absorbance of the initial solution of the free proton donor BH at the given wavelength. The rearranged form below is the well-known Benesi–Hildebrand equation,³⁰ which was used to estimate the ratio of chromophore–anion association.³¹ If the concentration of free anion Y[−] is much larger than that of the complexed anion (when a large excess of anion is used), [Y[−]] in equation 3 can be replaced by the overall anion concentration $c_{\text{Y}^-} = [\text{Y}^-] + [\text{LH} - \text{Y}^-] \approx [\text{Y}^-]$.

$$\frac{A_0}{A - A_0} = \frac{\epsilon_{\text{LH}}}{\epsilon_{\text{LH}\cdots\text{Y}^-} - \epsilon_{\text{LH}}} \left(\frac{1}{K_s[\text{Y}^-]^n} + 1 \right) \quad (3)$$

1,4-Bis(hexyloxy)-2,5-bis(6-*tert*-butylbenzoxazolyl)benzene (3b). 2,5-Bis(hexyloxy)teraphthalaldehyde (0.2500 g, 0.747 mmol) and 2-amino-4-*tert*-butylphenol (0.3700 g, 2.242 mmol) were heated to reflux in toluene (30 mL) under an argon atmosphere for 15 h. The intermediate imine product was collected by filtration and purified by recrystallization from methanol to give yellow crystals (0.4200 g, 89%). ¹H NMR (CDCl₃, 300 MHz, δ): 0.923 (t, $J = 7.0$ Hz, 6H, −CH₃), 1.368–1.580 (m, 30H, −CH₂−), 1.950 (m, 4H, −CH₂−), 4.167 (t, 4H, −OCH₂−), 6.981 (d, $J = 8.4$ Hz, 2H, Ar–H), 7.105 (s, br, 2H, Ar–OH), 7.280 (dd, $^3J = 8.4$ Hz, $^4J = 1.8$ Hz, 2H, Ar–H), 7.322 (d, $J = 1.8$ Hz, 2H, Ar–H), 7.726 (s, 2H, Ar–H), 9.189 (s, 2H, N=CH).

The intermediate imine product (0.40 g, 0.64 mmol) and DDQ (0.35 g, 1.6 mmol) were dissolved in a mixture of 5 mL of THF and 30 mL of methylene chloride. After stirring for 12 h, the reaction mixture was treated with a 1 N NaOH aqueous solution and methylene chloride to remove the DDQH byproduct, then washed with water and brine, and dried over Na₂SO₄. After evaporation of the solvent, the solid residues were collected and purified on a silica gel column by using an eluant (hexane:ethyl acetate = 5:1). After recrystallization from methanol, the product **3b** was obtained as an off-white solid (0.33 g, 83%; mp 149–151 °C). ¹H NMR (CDCl₃, 300 MHz, δ): 0.929 (t, $J = 6.6$ Hz, 6H, −CH₃), 1.372–1.590 (m, 30H, −CH₂−), 1.930 (m, 4H, −CH₂−), 4.235 (t, $J = 6.6$ Hz, 4H, −OCH₂−), 7.472 (dd, $^3J = 8.7$ Hz, $^4J = 1.8$ Hz, 2H, Ar–H), 7.539 (d, $J = 8.7$ Hz, 2H, Ar–H), 7.868 (d, $J = 1.8$ Hz, 2H, Ar–H), 7.885 (s, 2H, Ar–H). ¹³C NMR (CDCl₃, 75 MHz, δ): 14.307, 22.898, 25.947, 29.534, 31.814, 32.036, 35.215, 70.451, 109.451, 116.558, 116.826, 120.227, 123.304, 141.871, 148.301, 149.175, 152.078, 161.864. Anal. Calcd for C₄₀H₅₂N₂O₄: C, 76.89; H, 8.39; N, 4.48. Found: C, 77.20; H, 8.50; N, 4.50.

2,5-Bis(6-*tert*-butylbenzoxazolyl)hydroquinone (6). A solution of **3b** (0.29 g, 0.46 mmol) in 10 mL of dry methylene chloride was cooled with dry ice/acetone. BBr₃ in methylene chloride (1 M, 1.4

(34) Vass, A.; Dudas, J. Z.; Toth, J.; Varma, R. S. *Tetrahedron Lett.* **2001**, 42, 5347–5349.

(35) Lakowicz, J. R. *Principles of Fluorescence Spectroscopy*; Kluwer Academic: New York, 1999; pp 51–55.

(36) The absorption λ_{max} for **5** and its monoanion is calculated to be 367 and 489 nm, respectively. *HyperChem for Windows*, release 7.5; Hypercube, Inc.: Gainesville, FL.

mL) was added dropwise under an argon atmosphere. The reaction mixture was stirred at $-78\text{ }^{\circ}\text{C}$ for 2 h and then at room temperature overnight. Following the addition of 2.0 mL of distilled water, the reaction mixture was stirred for additional 2 h and poured into a mixture of water (20 mL) and methylene chloride (10 mL). The organic layer was separated, and the aqueous layer was extracted twice with methylene chloride (20 mL). The combined organic layer was washed with brine and dried over anhydrous MgSO_4 . After removal of the solvent on a rotary evaporator, the crude product was purified by recrystallization from methanol, which gave **6** as yellow crystals (0.19 g, 90% yield, mp $354\text{--}355\text{ }^{\circ}\text{C}$). ^1H NMR (CDCl_3 , 300 MHz, δ): 1.441 (s, 18H, CH_3), 7.510 (dd, $^3J = 8.7\text{ Hz}$, $^4J = 1.8\text{ Hz}$, 2H, Ar-H), 7.586 (d, $J = 8.7\text{ Hz}$, Ar-H), 7.790 (s, 2H, Ar-H), 7.802 (d, $J = 1.8\text{ Hz}$, Ar-H), 11.128 (s, 2H, Ar-OH). ^{13}C NMR (CDCl_3 , 75 MHz, δ): 31.974, 35.281, 110.267, 114.689, 114.903, 116.277, 124.068, 140.219, 147.611, 149.192, 151.178, 162.213. Anal. Calcd for $\text{C}_{28}\text{H}_{28}\text{N}_2\text{O}_4$: C, 73.66; H, 6.18; N, 6.14. Found: C, 73.46; H, 6.24; N, 6.04.

1,4-Bis(hexyloxy)-2,5-bis(6-bromobenzoxazolyl)benzene (3a). Compound **3a** (30% yield, mp $170\text{--}172\text{ }^{\circ}\text{C}$) was synthesized from 2-amino-4-bromophenol by following the same procedure as that for **3b**. ^1H NMR (CDCl_3 , 300 MHz, δ): 0.886 (t, 6H, $-\text{CH}_3$), 1.248–1.596 (m, 12H, $-\text{CH}_2-$), 1.912 (m, 4H, $-\text{CH}_2-$), 4.220 (t, $J = 6.4\text{ Hz}$, $-\text{OCH}_2-$), 7.465 (d, $J = 8.4\text{ Hz}$, Ar-H), 7.510 (dd, $^3J = 8.4\text{ Hz}$, $^4J = 2.0\text{ Hz}$, 2H, Ar-H), 7.856 (s, 2H, Ar-H), 7.945 (d, $J = 2.0\text{ Hz}$, 2H, Ar-H). ^{13}C NMR (CDCl_3 , 75 MHz, δ): 14.295, 22.886, 25.927, 29.449, 31.761, 70.366, 112.072, 116.457, 117.579, 119.826, 123.336, 128.587, 143.564, 150.066, 152.175, 162.654. Anal. Calcd for $\text{C}_{32}\text{H}_{34}\text{Br}_2\text{N}_2\text{O}_4$: C, 57.33; H, 5.11; N, 4.18. Found: C, 56.81; H, 5.15; N, 4.10.

Synthesis of Polymer 4. A solution of **3a** (0.1365 g, 0.2036 mmol) and 9,9-dihexylfluorene-2,7-bis(trimethyleneborate) (0.1023 g, 0.2036 mmol) in toluene (15 mL) was degassed and filled with argon. Following the addition of an aqueous K_2CO_3 solution (2 M, 5 mL) and $\text{Pd}(\text{PPh}_3)_4$ (110 mg, 5 mol %), the reaction mixture was heated to reflux for 24 h under an argon atmosphere. The product solution was poured into acidic methanol (200 mL), and the crude polymer was precipitated and collected by centrifuge. The obtained polymer was redissolved in THF (10 mL), and the resulting solution was added into methanol (200 mL) to precipitate the polymer. After three cycles of dissolution–precipitation were repeated, the purified polymer was collected and dried at $40\text{ }^{\circ}\text{C}$ under vacuum for 24 h. The polymer **4** (0.145 g, 84.4%) was a brown powder with a

number-average molecular weight (M_n) of 22 800 g/mol (PDI = 1.70). ^1H NMR (CDCl_3 , 300 MHz, δ): 0.794–1.659 (m, $-\text{CH}_2-$ and $-\text{CH}_3$), 1.956–2.083 (m, 8H, $-\text{CH}_2-$) 4.307 (s, br, 4H, $-\text{OCH}_2-$), 7.671–8.137 (m, 14H, Ar-H). Anal. Calcd for $\text{C}_{57}\text{H}_{66}\text{N}_2\text{O}_4$: C, 81.20; H, 7.98; N, 3.32. Found: C, 79.28; H, 7.89; N, 3.07.

Synthesis of Polymer 5. A solution of polymer **4** (0.100 g) in 10 mL of dry methylene chloride was cooled under an argon atmosphere with dry ice in acetone. Then a solution of BBr_3 in methylene chloride (1 M, 2.0 mL) was added dropwise via a syringe. The mixture was stirred at $-78\text{ }^{\circ}\text{C}$ for 2 h and then at room temperature overnight. After the addition of 2.0 mL of distilled water, the reaction mixture was stirred for an additional 2 h and transferred into a separation funnel containing water (20 mL) and methylene chloride (10 mL). The organic layer was separated, and the aqueous layer was extracted with methylene chloride (20 mL). The combined organic layer was washed with brine and dried over anhydrous MgSO_4 . The polymer was precipitated by the addition of the concentrated solution (about 10 mL) into 200 mL of methanol and collected by a centrifuge. The polymer was redissolved in THF (10 mL), and the resulting solution was added dropwise into methanol (200 mL). The cycle of redissolution–precipitation was repeated three times. After drying at $40\text{ }^{\circ}\text{C}$ under vacuum for 24 h, the polymer **5** (0.043 g, 53.2%) was obtained as a reddish powder, which has the following spectral properties. The polymer **5** was soluble in THF, slightly soluble in chloroform, but insoluble in methanol. ^1H NMR (CDCl_3 , 300 MHz, δ): 0.687–0.95 (br, 10H, $-\text{CH}_2-$ and $-\text{CH}_3$), 1.00–1.360 (m, 12H, $-\text{CH}_2-$), 2.00–2.023 (br, 4H, $-\text{CH}_2-$), 7.521–7.90 (m, 12H, Ar-H), 8.079 (s, 2H), 11.070 (br, 2H, Ar-OH).

Acknowledgment. Financial support has been provided by NASA (Grant NNC06AA20A) and The University of Akron. We also thank Professor Wesdemiotis at The University of Akron for his helpful suggestion and assistance in acquiring MS of the model compound.

Supporting Information Available: ^1H NMR spectra of **4** and **5**, SEC chromatography of **4**, X-ray structural information on **6**, and IR spectra of **5** and **6**. This material is available free of charge via the Internet at <http://pubs.acs.org>.

CM0713982